Engineered hierarchical microdevices enable pre-programmed controlled release for postsurgical and unresectable cancer treatment

Lihuang Wu, Junhua Li, Yuqi Wang, Xinyue Zhao, Yiyan He, Hongli Mao, Wenbo Tang, Rong Liu, Kui Luo, and Zhongwei Gu**

L. Wu, J. Li, Y. Wang, X. Zhao, Y. He, H. Mao, Z. Gu

Research Institute for Biomaterials, Tech Institute for Advanced Materials, College of Materials Science and Engineering, Jiangsu Collaborative Innovation Center for Advanced Inorganic Function Composites, Suqian Advanced Materials Industry Technology Innovation Center, Nanjing Tech University, Nanjing 211816, China

Y. He, H. Mao, Z. Gu

NJTech-BARTY Joint Research Center for Innovative Medical Technology, Nanjing Tech University, Nanjing 210009, China

W. Tang, R. Liu

Faculty of Hepatopancreatobiliary Surgery, the First Medical Center, Chinese PLA General Hospital, Beijing 100039, China.

K. Luo, Z. Gu

Department of Radiology, Huaxi MR Research Center (HMRRC), National Clinical Research Center for Geriatrics, Frontiers Science Center for Disease-Related Molecular Network, State Key Laboratory of Biotherapy, West China Hospital, Sichuan University, Chengdu 610041, China.

J. Li

This article has been accepted for publication and undergone full peer review but has not been through the copyediting, typesetting, pagination and proofreading process, which may lead to differences between this version and the Version of Record. Please cite this article as doi: 10.1002/adma.202305529.

Technique Center, Jinling Pharmaceutical Company Limited, Nanjing 210046, China

E-mail: h.mao@njtech.edu.cn; zwgu@scu.edu.cn; zwgu@njtech.edu.cn

Keywords: microfabrication, hierarchical microstructure, surface erosion, pre-programmed controlled release, postsurgical treatment, unresectable tumor control

Abstract

Drug treatment is required for both resectable and unresectable cancers to strive for any meaningful patient outcomes improvement. However, the clinical benefit of receiving conventional systemic administrations is often less than satisfactory. Drug delivery systems are preferable substitutes but still fail to meet diverse clinical demands due to the difficulty in programming drug release profiles. Herein, we introduce a microfabrication concept, termed Hierarchical Multiple Polymers Immobilization (HMPI), and engineer biodegradable polymers-based hierarchical microdevices (HMDs) that can pre-program any desired controlled release profiles. Based on the first-line medication of pancreatic and breast cancer, controlled release of single gemcitabine and the doxorubicin/paclitaxel combination in situ for multiple courses was implemented, respectively. Preclinical models of postsurgical pancreatic, postsurgical breast, and unresectable breast cancer were established, and the designed hierarchical microdevices demonstrated well-tolerable and effective treatments for inhibiting tumor growth, recurrence, and metastasis. The proposed HMPI strategy allows us to create tailorable and high-resolution hierarchical microstructures for pre-programming controlled release according to clinical medication schedules, which may provide promising alternative treatments for postsurgical and unresectable tumor control.

1. Introduction

Surgery is the mainstay of clinical cancer treatment and remains the only option for cure for most malignant solid tumors. Perioperative (neoadjuvant or adjuvant) therapy further improves patient outcomes by either shrinking the tumor sufficiently to allow surgery or eradicating dormant minimal

residual disease (MRD) and micrometastases to prevent disease recurrence, establishing a standard of care for localized resectable disease.[1] In parallel, despite improvements in diagnostic techniques, a part of advanced or elderly patients with unresectable tumors suffer from poor physical condition and are advocated palliative treatment to control symptoms and extend life.[2] For these treatments, systemic administration of antitumor drugs is the most prevalently taken approach as chemotherapy, immunotherapy, endocrine therapy, and gene therapy.[3] However, drug molecules are largely unspecific and have difficulty achieving desired accumulation at the tumor site to produce effective responses, which can result in severe systemic toxicity, irreversible drug resistance, and undesirable patient outcomes.[4]

Tremendous efforts have been contributed to overcoming the pharmacokinetic limitations of antitumor drugs, especially the emergence of cancer nanomedicines. Unfortunately, the harsh physical and physiological barriers that nanoparticles face after intravenous injection also limit their delivery efficiency to target sites.[5] Study revealed that only 0.7% (median) of the injected dose (ID) of the nanoparticles developed in the past were successfully delivered to solid tumors,[6] which explains why these decades saw such a block in the translational progress of cancer nanomedicines. Alternatively, implantation or injection of localized devices represents another promising option to the conventional systemic administration.[7] These devices are designed to release therapeutic agents directly to the disease site by in-situ implantation or injection, thus offering strategies for eliminating localized disease and preventing distant metastasis. Clinically available products, such as Gliadel® Wafer and Zoladex®, are characterized by simple homogeneous structures and can only provide sustained drug release.[8] However, clinical administration regimens require strict adherence to specific medication schedules. Proper medication time, repeated administration, multiple courses, and drug combination are increasingly needed for optimal oncological outcomes (**Scheme 1**a), which poses a challenge to the development of antitumor localized devices.

Advanced microfabrication techniques (e.g., additive manufacturing,[9] microfluidics,[10] electrospinning,[11] and soft lithography[12]) have contributed significantly to creating devices with heterogeneous structures. Henceforth the drugs have been designed to be released from the devices in diverse controlled manners (e.g., rate-controlled,[9a, 10a, 13] pulsatile,[12b, 12c] sequential,[10b, 11b, 11c, 14] and on-demand[15]). However, these techniques have either subjected to a compromise between

resolution and the materials that can be used or failed in fabricating reliable complex microstructure.[12d, 16] On the other hand, biodegradable aliphatic polyesters such as poly(lactic-co-glycolic acid) (PLGA) are recognized the favorite drug carriers due to their extensive clinical practice experience. However, they are associated with many unsolved problems, such as non-linear degradation due to their bulk-degrading nature,[17] which makes these materials applicable to only a subset of drug controlled release profiles (e.g., sustained[18] and pulsatile[12b, 12c]). Therefore, it remains a significant problem and challenge to design controlled release devices in responding to the clinical administration requirements, which demonstrates the critical need for a more rational fabrication technique, structure, and material.

In this work, we describe a customizable and precisely controllable hierarchical polymer microfabricating concept to create devices that enable drugs to release in pre-programmed controlled manners. Our strategy, which is termed Hierarchical Multiple Polymers Immobilization (HMPI), allows multiple drug-loaded polymer formulas to be combined by pre-design to generate hierarchical microdevices (HMDs) with highly controllability at high resolution. The created HMDs enable the embedded drugs to be released as the surface erosion of polymers. Hence, a new paradigm of drug pre-programmed controlled release (PPCR) in situ at the tumor site can be achieved by tailoring the hierarchical microstructures of the HMDs (Scheme 1b).

Through this strategy, we can obtain any desired drug release profiles according to clinical needs, and for the first time, we successfully implemented multiple courses of single-drug and multi-drug controlled release in situ (Scheme 1c-e). Based on the first-line medication of pancreatic and breast cancer, the HMDs were engineered to provide multi-course controlled release of 1) gemcitabine for monotherapy and 2) doxorubicin and paclitaxel for combination therapy, respectively. The antitumor effects and biosafety of the designed HMDs were evaluated using preclinical postsurgical and unresectable cancer models. The HMPI strategy thus offers the possibility of customizing and optimizing controlled drug release through pre-programmed design and precise microfabrication, representing potential alternatives to dealing with postsurgical and unresectable tumors.

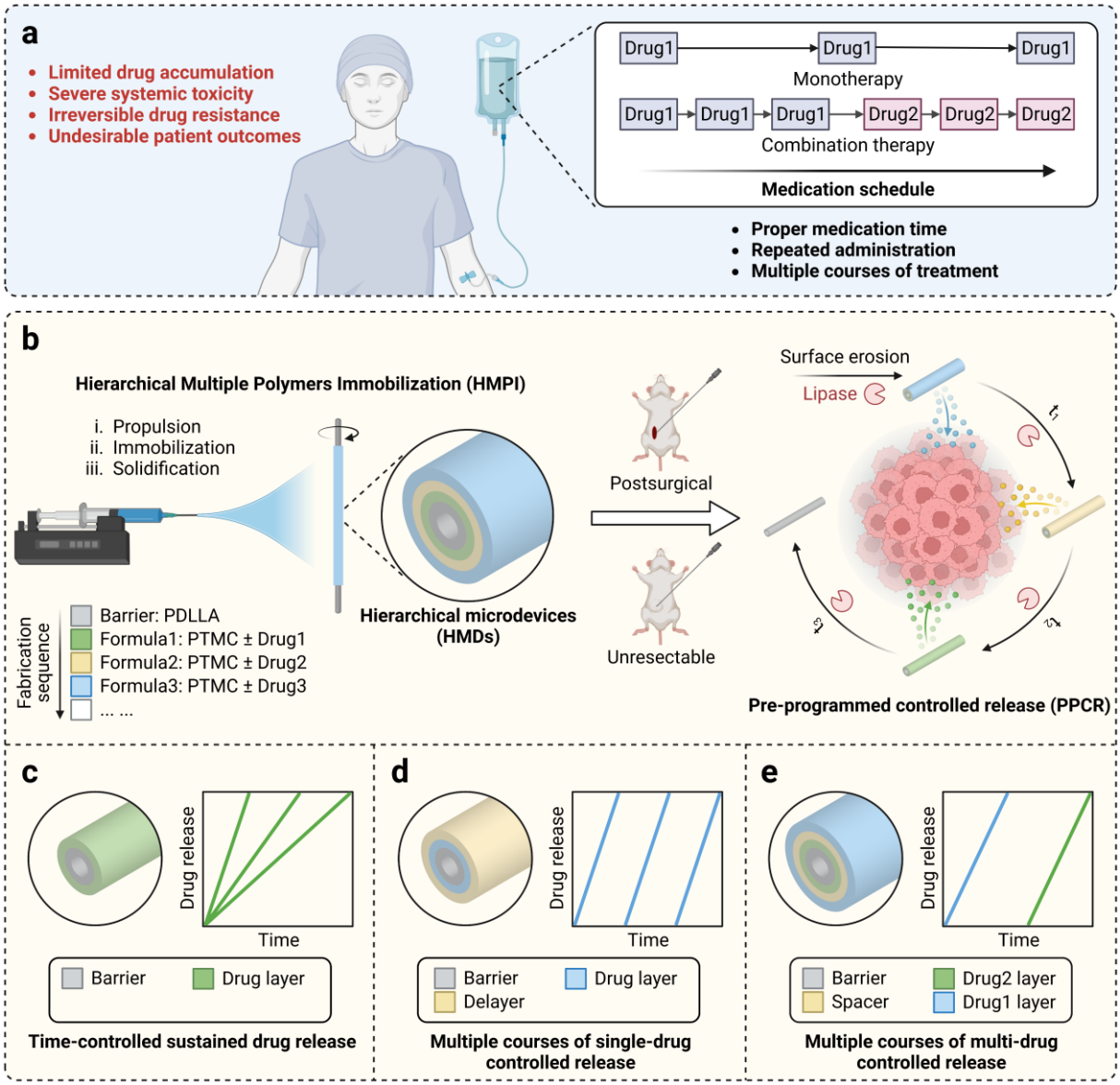

Scheme 1. Schematic illustration of the design and application of HMPI concept to engineer HMDs for pre-programmed controlled release under the guidance of clinical medication schedules. a) General medication schedules of clinical oncology treatment. b) Design and fabrication of HMDs via HMPI strategy to pre-program controlled release in situ for postsurgical and unresectable cancer treatment (demonstrated using HMD with the internal PDLLA barrier and three external PTMC ± Drug layers as an example). c-e) Applicable controlled release profiles via HMPI strategy.

2. Results and Discussions

2.1. Design and application of HMPI concept to fabricate HMDs

As shown in Scheme 1b, the HMPI concept was performed to fabricate HMDs through a modified electrospinning processing approach, in which the polymeric formulas were ejected, driven by a high electric field, and concentrically collected and immobilized onto a rotating mini-size stainless-steel mandrel. HMDs with custom-made microstructures can thus be created by changing the feeding formula, volume, and sequence. In particular, FDA-approved biodegradable polymers were used to construct the HMDs. Poly(DL-lactide) (PDLLA, number-average molecular weight M_n = 120 kDa, Figure S1a, Supporting Information) with a long-term degradation behavior (detectable weight loss takes over 7 weeks at 37 °C and pH 7.4[19]) is taken as the supporting base and barrier by the merit of its high strength and extremely low permeability to various drugs.[20] High molecular weight poly(trimethylene carbonate) (PTMC, M_n = 430 kDa, Figure S1b, Supporting Information) with a intriguing surface erosion behavior is used to embed drugs and control their release.[21] In this scenario, surface erosion of the PTMC matrix is expected to occur uniquely and unilaterally on the external surface of HMDs due to the internal PDLLA barrier and large length-diameter ratio, subsequently releasing the embedded drugs.

An HMD with the most basic structure was constructed by electrosprayed PDLLA microparticles (Figure S2a, Supporting Information) as the internal layer and electrospun PTMC nanofibers (Figure S2b, Supporting Information) as the external one. The immobilized HMD with a porous morphology was incubated in the heating vacuum for further drying and solidification, where PDLLA microparticles and PTMC nanofibers were easily fused into dense matrice due to their high specific surface areas (**Figure 1**a). Subsequently, the solidified hierarchical sample was demoulded and cut into 10 mm-long tubular HMDs. A clear-cut distinction between layers could be observed by scanning electron microscope (SEM, Figure 1b), indicating the generation of hierarchical microstructures of multiple polymers. The experimentally determined relationship among length, layer thickness, and mass of HMDs was found to agree well with the theoretically calculating equation (Figure S3, Supporting Information), suggesting the high controllability and resolution of the process.

Hydrolytic enzymes, especially lipases, have previously been confirmed by our group to be responsible for the biodegradation of PTMC and have been used to mimic the in vivo degradation of PTMC.[21-22] Lipase solution (1000 U/mL) was used to evaluate the degradation performance of HMDs, as PTMC in it showed rapid degradation similar to that in vivo.[22-23] The results (Figure 1c and d) show that a unilateral surface erosion occurred uniquely on the external PTMC surface of HMDs. Significantly, this unique heterogeneous erosion on the PTMC layer followed a linear trend (Figure 1e) as calculated from the SEM images. Determining from the chemical composition evolution (Figure 1f), the PTMC weight ratio in HMDs during the surface erosion was also found to decrease linearly with time (Figure 1g). In addition, the samples were subcutaneously injected in mice, and the in vivo erosion on the HMDs indicates a similar phenomenon (Figure S4 and S5, Supporting Information). Despite significant erosion in vivo, the shape of the PDLLA supporting base of retrieved HMDs remained unchanged (Figure S4, Supporting Information), and the tubular body was adequate to resist the dynamic deformation caused by tissue pressure of the body, suggested by a cycling compression test mimicking the in vivo environment (Figure 1h and Figure S6, Supporting Information).

Drug permeability (i.e., diffusion) through polymers is an essential but often overlooked parameter that significantly affects the performance of drug delivery systems.[24] Hence, drug permeability through prepared PDLLA and PTMC was evaluated using Franz diffusion cell via Fick's first law.[20c, 25] Experiments on several antitumor agents, e.g., gemcitabine (GEM), doxorubicin hydrochloride (DOX), paclitaxel (PTX), and irinotecan hydrochloride (CPT-11) were performed herein. As a result, the permeation of these drugs through PDLLA and PTMC was found to be negligible, as their permeation coefficients were calculated to be extremely low (Table S1, Supporting Information). Based on these findings, we reason that these drugs released from a dense PDLLA or PTMC matrix are primarily governed by material degradation rather than drug diffusion.

We next examined the hierarchical microstructures of HMDs. Coumarin 6 (C6) and DOX, as the model drugs, were loaded in the PTMC matrix to construct HMDs with different hierarchical structures for imaging. Observing from fluorescence images of the cross sections (Figure 1i-l), each drug was distributed uniformly in its loading layer. In addition, the PDLLA barrier and pure PTMC layers (Figure 1j and l) adjacent to the drug-loading layers showed minimal fluorescence. The above results demonstrate the successful fabrication of HMDs with well-defined and independent hierarchical

microstructures. Combined with the unilateral surface erosion characteristic of HMDs and limited drug permeation through polymers, the engineered HMDs via the HMPI strategy are supposed to realize the unique PPCR profiles of drugs by tailoring the formulas of multilayers.

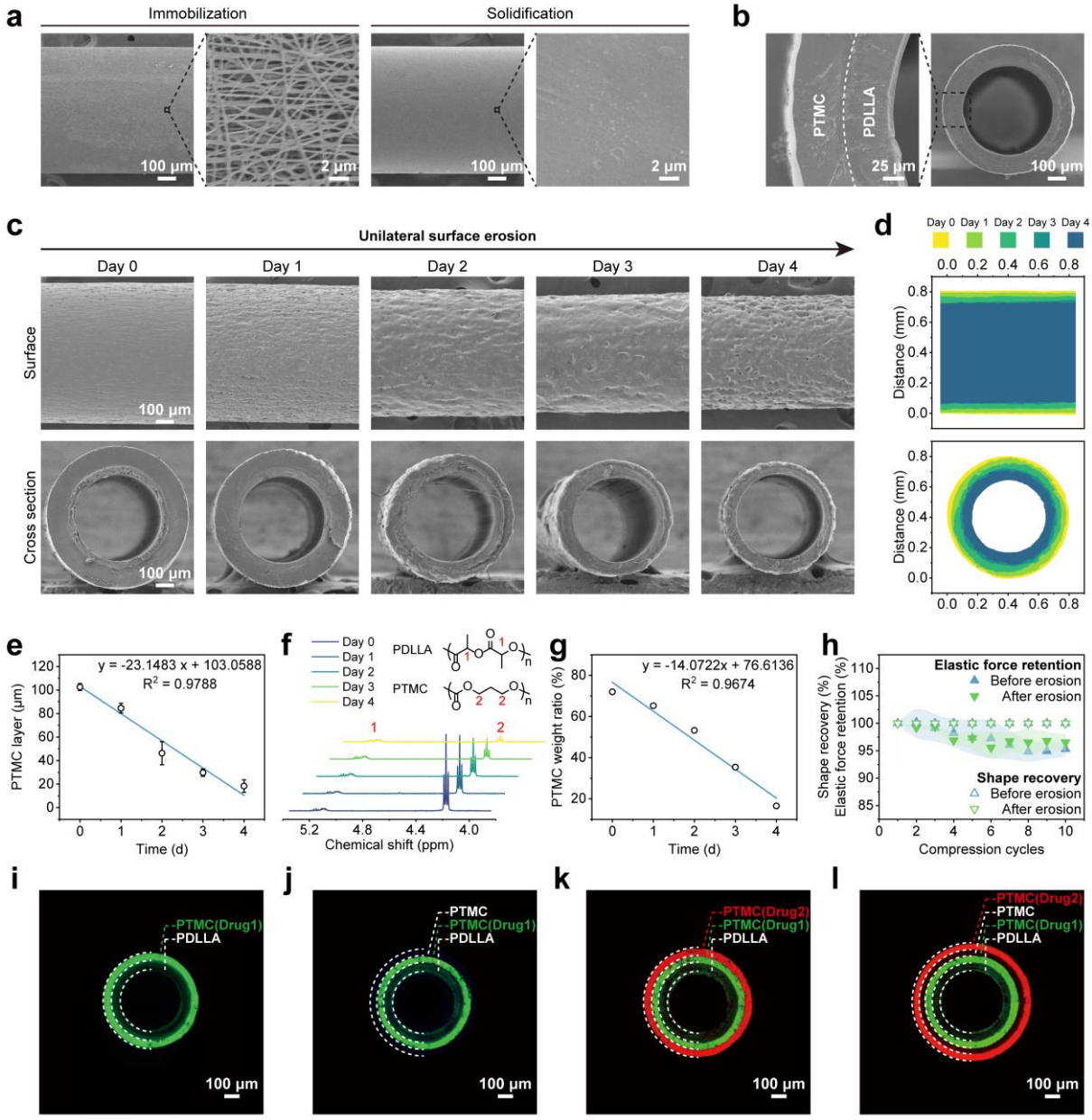

Figure 1. Morphology, degradation, and characterization of HMDs. a) Morphologies of a representative HMD after immobilization and solidification. b) The cross-section of the HMD with a

basic structure. c) Observation and d) schematic presentation of the surface erosion process of HMDs in vitro. e) Quantitative analysis of the thickness evolution of the PTMC layer. f) ^{1}H NMR spectra and g) chemical composition evolution of HMDs during the in vitro degradation. h) Cycling compression test of the HMDs in mimicking the in vivo implantation environment. i-l) Fluorescence images of the HMDs (model drug1: C6, model drug2: DOX). Data represent mean ± s.d. of n = 3 independent samples.

2.2. In vitro PPCR performance of HMDs

The pre-programming performance on drug-controlled release (i.e., PPCR) of the fabricated HMDs was assessed in vitro. The HMDs with DOX-loaded PTMC as the drug layers were incubated separately in Hank's and lipase (1000 U/mL) solution. They showed minimal DOX release in Hank's solution (Figure S7a and b, Supporting Information) as PTMC is nondegradable in this situation.[22] In contrast, significantly enhanced DOX release from the PTMC matrix could be found in lipase solution (Figure S7c, Supporting Information). The drug release data were further analyzed using representative drug release kinetic models, and the results (Table S2, Supporting Information) show that drug release from the HMDs was very closed to the zero-order kinetics. In addition, the Korsmeyer-Peppas model was used to describe the drug release mechanism. The fitting results indicate a typical erosion-diffusion mechanism when the drug-loading rate was ≤ 10%, and the erosion-mediated mechanism gradually became dominant as the drug-loading rate decreased. HMDs with drug layers of 50-200 μm were fabricated subsequently, and they could provide time-controlled sustained drug release for varied durations, pre-programmed by the drug layer thickness (**Figure 2**a, b and Scheme 1c). The calculated release exponents (n values) of the Korsmeyer-Peppas equation were found to be close to 1 (Table S3, Supporting Information), suggesting a polymer erosion-dominated drug release behavior. In general, drug release from a matrix system can not follow the ideal zero-order kinetics.[26] However, benefiting from the high resolution of the built drug layer and the unique polymer erosion-controlled drug release mechanism, HMDs generated via the HMPI strategy encouragingly provide almost zero-order constant release, which can facilitate the establishment of a predictable controlled release system.

Benefiting from the surface erosion behavior, pure PTMC was designed as a delayer to cover the drug layer (Scheme 1d). The starting time of drug release was found to be a function of delayer's

thickness (Figure 2c and d). In that scenario, the drug began to release only when the external delayer was eroded. Furthermore, HMDs that could provide controlled multi-drug release were engineered by loading different drugs in the outer and internal layers (Scheme 1e). In these cases, PTMC matrices of different thicknesses were inserted between these two drug layers as a spacer. The results showed that DOX (Drug1) and MB (Drug2) were sequentially released from the HMDs, strictly following the physically designed internal microstructures (Figure 2e). The PTMC spacers, which deployed an interval between the release profiles of different drugs, were also found to be programmable on the interval time by their thickness (Figure 2f).

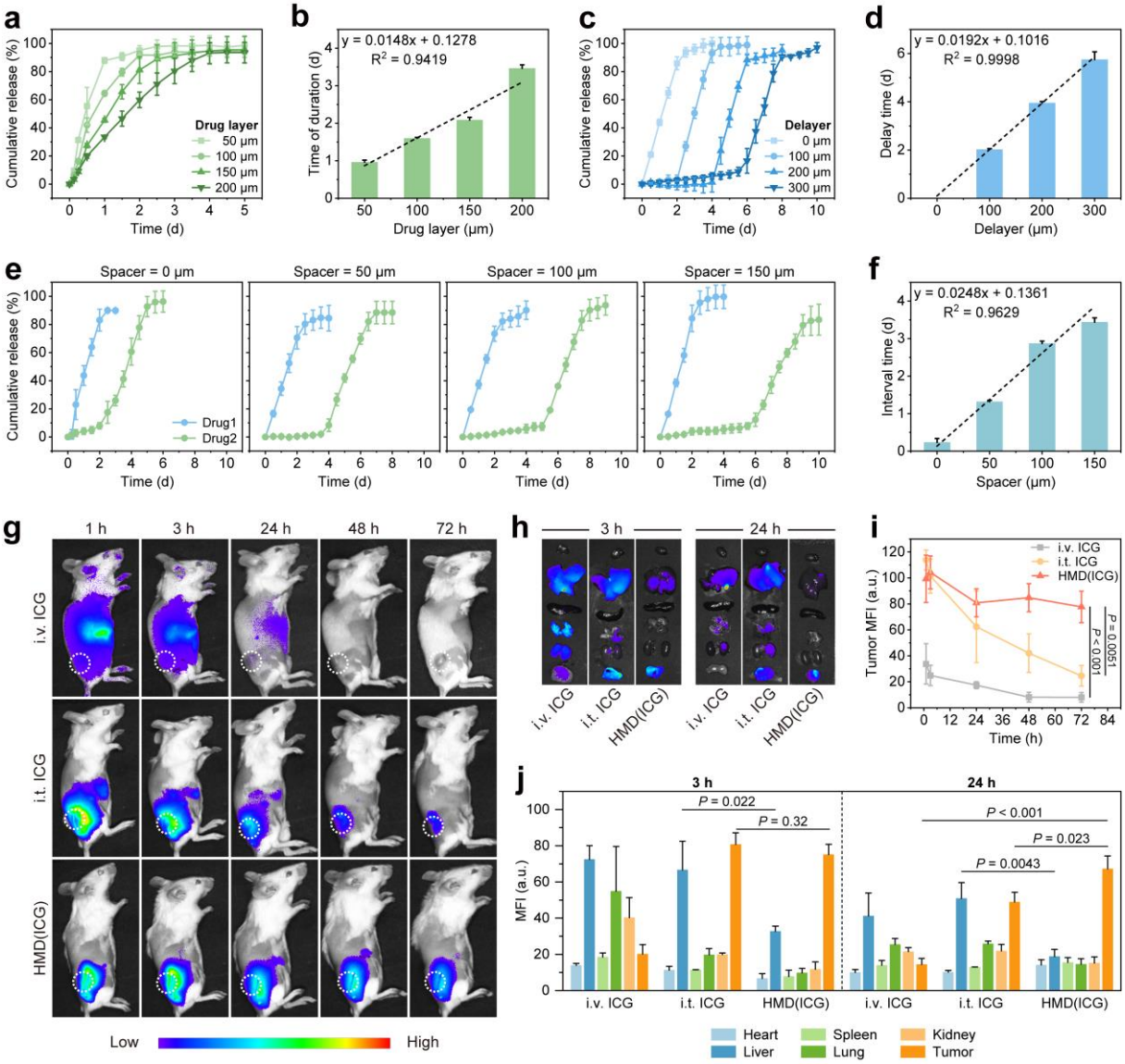

Figure 2. In vitro PPCR profiles and in vivo localized delivery performance of the HMDs. a) Time-controlled sustained drug release profiles and b) the relationship between drug release time of duration and drug-loading layer thickness (model drug: DOX). c) Time-delayed drug release profiles and d) the relationship between delay time and delayer thickness (model drug: DOX). e) Controlled multi-drug release profiles and f) the relationship between interval time and spacer thickness (model drug1: DOX, model drug2: methylene blue (MB)). Representative fluorescence images depicting the g) in vivo (white dotted circle indicates the tumor site) and h) ex vivo (top to bottom: heart, liver,

spleen, lung, kidney and tumor) biodistribution of model drug ICG in mice. i) Tumor mean fluorescence intensity (MFI) of in vivo fluorescence images. j) MFI of ex vivo fluorescence images (3 and 24 h after treatment). For a-f, i and j, data represent mean ± s.d. of n = 3 independent samples. For data in b, d, and f, linear fitting was applied.

The above results demonstrate that the HMDs primarily constructed by the surface-eroding PTMC provide unique and versatile tools for pre-programming controlled drug release. To evaluate the delivery performance of HMDs, a fluorescent dye indocyanine green (ICG)-labeled HMD, denoted as HMD(ICG), was prepared and subcutaneously injected (3 mg/kg) proximal to the tumor of a subcutaneous (s.c.) 4T1 breast tumor mouse model and monitored by an in vivo imaging system (Figure 2g and h). Compared to the intravenous (i.v.) injection group (i.v. ICG), HMD(ICG) showed greatly enhanced localized fluorescence signal at the tumor site with a minimized off-target effect (Figure 2i and j). In addition, intratumoral (i.t.) injection of free drug (i.t. ICG), despite initially providing high intratumoral drug levels, experienced a rapid fluorescence signal decay (Figure 2i). After the rapid absorption of i.t. ICG, drug metabolism also produced a great burden on the body (for ICG mainly from the liver, Figure 2h and j). HMD(ICG) also outperformed i.v. ICG because it releases drug that maintained a stable high intratumoral concentration for a long time with minimal body burden (Figure 2i and j). Thus, by pre-designing the hierarchical microstructure, an elaborate HMD is supposed to serve in-situ PPCR in the tumor bed.

2.3. Engineering HMDs enabling in-situ PPCR of GEM for pancreatic tumor treatment

As the HMPI strategy enables HMDs to release the drug in time-delayed manners (Figure 2c and d), a single drug can thus be designed to release at different time points for multiple courses by applying the combination of several HMDs with varied delayer thicknesses, which can mimic the clinical multiple courses of administration schedule.

Single-drug GEM remains the standard first-line treatment for pancreatic cancer. However, this compound suffers from rapid metabolism and inefficient delivery to the solid tumor, which

necessitates a high dose and repeated administration for multiple courses.[27] Conventional devices that present sustained release can thus find a problem in delivering GEM as a low dose may induce drug resistance while a high dose increases toxicity. To solve this, GEM was pre-programmed to release in situ for multiple courses by tailoring the microstructures of HMDs. By design, PTMC was used as the delayer, and the GEM-loaded PTMC matrix was embedded in HMDs as the cored GEM layer (Figure S8a, Supporting Information). The loaded GEM showed representative burst release profiles in vivo within two days probably due to the phase-separating nature of GEM-loaded PTMC matrix (Figure S8b and c, Supporting Information). The HMDs covered with PTMC delayer showed thickness-programmed delayed drug release profiles (Figure S8d and e, Supporting Information). Particularly, three HMDs varied in delayer thickness that enable multiple courses of GEM release, denoted as HMD(G), were combined and treated as one dose for one shot (30 mg/kg for 20 g mice). When subcutaneously injected at the same site in mice, these bundled-HMDs typically provided three courses of GEM release in situ (at day 0, 4, and 9, respectively, **Figure 3**a and b).

The body weight analysis showed excellent biosafety of HMD(G) treatment. In comparison, the mice treated with a PLGA-based matrix device that provided representative sustained GEM release at the same dose were found to experience diarrhea and lose their body weight dramatically (Figure S9 and S10, Supporting Information). Despite the popularity of sustained-release devices for the delivery of a variety of antitumor drugs, it seems that the release profile of GEM requires programmed optimization according to the clinical schedule. This may be because the highly polymorphic cytidine deaminase (CDA), which is responsible for the liver elimination and detoxification of GEM, is prone to deregulation upon continuous exposure to GEM, resulting in erratic GEM pharmacokinetics and severe adverse drug reactions.[28] As a result, prolonged administration of GEM can produce higher toxicity than rhythmic bolus administration.[29] The tolerated dose level of the HMD(G) regimen outperformed the conventional device with sustained GEM release, suggesting a greater therapeutic effect as a more extensive in-situ release can be achieved by HMD(G) treatment. Upon HMD(G) injection, GEM biodistribution was examined. The results show that high drug retentions in pancreatic tumors (up to 123 μg/g) were achieved periodically on the days of GEM release (Figure 3c). In-situ release of GEM by HMD(G) in mice resulted in 17.1-fold greater local drug concentrations and up to 24.5-fold lower systemic drug levels than the i.v. injection of free drug (Figure 3d).

The antitumor effect was evaluated using a postsurgical Panc02 pancreatic tumor mouse model (Figure 3e). Postsurgical implantation of HMD(G) (30 mg/kg, directly in the open surgical cavity) showed a significant tumor relapse inhibition in the mice, outperforming conventional i.v. GEM (denoted as G, 80 mg/kg) and the control arms of i.v. normal saline (denoted as NS) and blank hierarchical microdevice (denoted as HMD) over a 7-week postoperative observation (Figure 3f and g). The relapsed tumors were significantly minimized after HMD(G) treatment (Figure 3h and i). The histological slices further revealed significant destruction of tumor tissue and apoptosis of tumor cells, associated with decreased tumor cell proliferation (Figure S11, Supporting Information). By body weight analysis, HMD(G) treatment was better tolerated than the systemic administration (Figure 3j). Biochemical analysis of the serum of mice further indicates that HMD(G) treatment did not induce liver or kidney function abnormalities (Figure S12, Supporting Information). In addition, no apparent damage to body organs was found by hematoxylin and eosin (H&E) staining (Figure S13, Supporting Information). The mice treated with HMD(G) showed significantly extended animal survival after surgery, with four of six remaining alive for 90 days (Figure 3k). Collectively, these results demonstrate that HMPI strategy successfully implemented in-situ controlled release of single-drug for multiple courses in responding to clinical monotherapy. Compared to the conventional sustained release device, the HMDs that were pre-programmed to release GEM in situ for optimized multiple courses exhibited greatly enhanced tolerance, resulting in significant inhibition of pancreatic tumor recurrence with excellent biosafety. Although the Panc02 tumor model does not totally represent human pancreatic cancer (e.g., differences in desmoplastic responses),[30] these preclinical results suggest that HMD(G) may be superior to clinical systemic administration, representing a promising safe and effective treatment for pancreatic cancer.

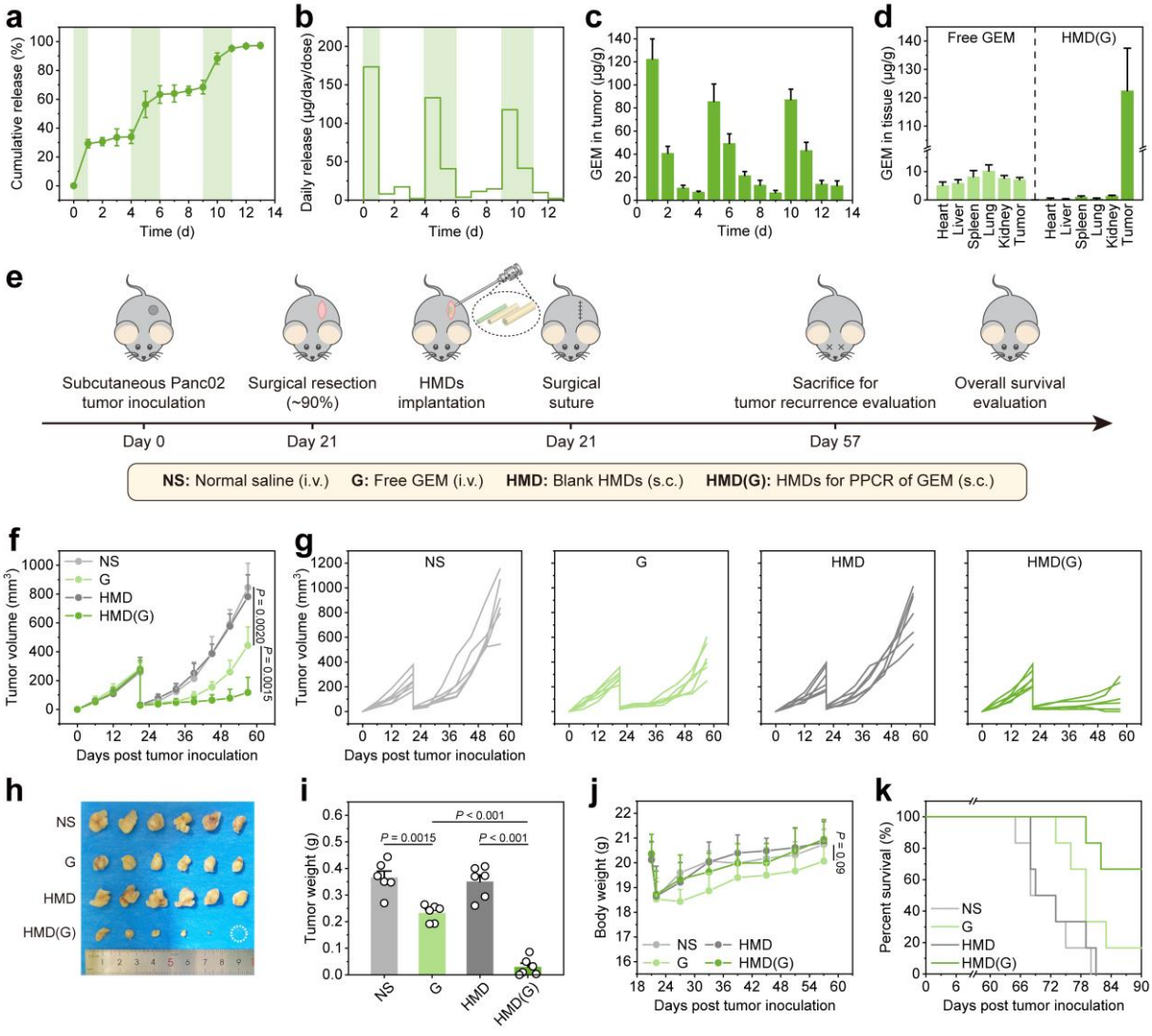

Figure 3. Engineering HMDs enabling in-situ PPCR of GEM for postsurgical pancreatic tumor treatment. In vivo a) cumulative and b) daily GEM release profiles of HMD(G). c) The GEM content in tumors upon HMD(G) injection. d) The GEM biodistribution of i.v. free GEM administration and s.c. HMD(G) injection. e) Treatment scheme of surgical resection and HMD(G) regimen in Panc02 tumor-bearing mice. f) Average and g) individual tumor growth kinetics. h) Image and i) weight of tumors after treatment. j) Body weight changes of mice after treatment. k) Animal survival curves. For a, c and d, data represent mean ± s.d. of n = 3 independent samples. For f and j, data represent mean ± s.d. of n = 6 independent samples. For i, data represent mean ± s.e.m. of n = 6 independent samples. Statistical significance was determined using the two-tailed unpaired *t*-test.

2.3. Engineering HMDs enabling in-situ PPCR of DOX and PTX for breast tumor treatment

As shown in Figure 2e and f, HMDs were capable of releasing multiple drugs in desired pre-programmed profiles. Multi-drug combinations represent more effective treatments but can result in more severe toxicity in clinical practice. For this, the HMPI strategy can be utilized to fabricate HMDs that can pre-program multiple drugs to release at reasonable time points and for desired courses, thus potentially avoiding the combined toxicity of multi-drug usage.

Sequential treatments based on anthracyclines and taxanes represent the most common choices for breast cancer management.[31] Abundant clinical experience has demonstrated that the sequential regimens are superior to the concurrent ones in the risk of recurrence, accompanied by lesser side effects such as hematologic and cardiac toxicity.[3, 32] In addition, a meta-analysis by the Early Breast Cancer Trialists' Collaborative Group (EBCTCG) has suggested that breast cancer patients can benefit from dose intensification by a more frequent administration or sequential scheduling.[33] Despite this, many patients can fail to complete the full courses of the longer sequential therapy regimens, which results in moderate therapeutic effects.[33] Hence, a system that enables continuous in-situ release of anthracyclines followed by taxanes at the tumor site can be conducive to improving patient compliance and eventually treatment outcomes.

Herein, the HMDs was pre-programmed via the HMPI strategy to provide multi-course controlled release of DOX and PTX in situ for breast tumor treatment. Firstly, in vivo drug release profiles of the HMDs loaded with DOX and PTX were investigated, respectively (Figure S14, Supporting Information). As DOX release from the PTMC matrix was found to take quite a long time, polyethylene glycol (PEG, 4000 Da) was composited with PTMC to enhance the drug diffusion (Figure S15, Supporting Information) in order to make it suitable for preclinical study at the animal level. Optimizing from these investigations, an HMD consisting sequentially of PDLLA barrier, PTX-loaded PTMC matrix (PTX layer), PTMC spacer, and DOX-loaded PTMC/PEG matrix (DOX layer) (Figure S16, Supporting Information) was preferably engineered for sequential DOX and PTX release. This particular HMD is denoted as HMD(A-T) according to the clinical sequential administration of anthracycline and taxane chemotherapy[33], in which the A represents adriamycin while the T represents paclitaxel. As a result,

HMD(A-T) provided in-situ sustained DOX release for around 6 days as a first course of treatment. The designed PTMC spacer encouragingly deployed a 4-day interval to imitate the dosing rest in medication schedules. Sequentially, 84.5% of the embeded PTX was released from the PTX layer as the subsequent course (**Figure 4**a and b). Localized application of the HMD(A-T) (at the dose of DOX 5 mg/kg and PTX 15 mg/kg) was capable of maintaining high levels of DOX (up to 24.8 μg/g) and PTX (up to 47.7 μg/g) in a programmed sequence in the tumors (Figure 4c), greatly exceeded the control arms of i.v. DOX and PTX administration by 5.9 and 12.3 fold, respectively (Figure 4d). Meanwhile, upon HMD(A-T) injection, both DOX and PTX concentrations in the off-target organs were detected to be limited, indicative of weakened systemic toxicity.

A postsurgical 4T1 breast tumor mouse model was established to evaluate the anti-recurrence effect of HMD(A-T) treatment (Figure 4e). Dose-gradient antitumor experiments were performed first, and HMD(A-T) showed dose-dependent antitumor effects and biosafety (Figure S17, Supporting Information). At an optimized dose, HMD(A-T) treatment was further evaluated against systemic chemotherapy regimens. Systemic administration of DOX (5.00 mg/kg) and PTX (15.00 mg/kg) concurrently (denoted as AT according to clinical concurrent administration of anthracycline and taxane chemotherapy[33]) and sequentially (denoted as A-T according to clinical sequential administration of anthracycline and taxane chemotherapy[33]) showed similar and moderately suppressed tumor growth curves (Figure 4f-i), however, at a price of a highly toxic side-effect by body weight analysis (Figure 4j). In comparison, HMD(A-T) treatment (DOX/PTX = 5.00/15.0 mg/kg) exhibited observably enhanced inhibition on tumor recurrence, with three of six mice's residual tumors being completely suppressed (Figure 4h and i). The antitumor effect of this multi-course controlled release of DOX and PTX in situ was slightly enhanced than a corresponding concurrent regimen, i.e., HMD(AT) (Figure S18, Supporting Information). Although the result did not reach significance, the advantage of HMD(A-T) treatment compared to HMD(AT) may lie in the fact that it offers an optimized and relatively prolonged regimen with high local drug concentrations. As suggested by substantial clinical experience, the outcome of administering high quantities of chemotherapeutic drugs at the beginning of treatment may be undesirable because higher doses of drugs do not necessarily improve cancer cell killing and may lead to unbearably high toxicity.[34] Optimizing the schedule represents the implication of maximizing drug combination effect with

minimal toxicity. As a result, HMD(A-T) showed more prominent biosafety during treatment compared to the HMD(AT) group, based on greater body weight gain (Figure 4j). No observable damage was found in the main organs of mice after treatment (Figure S19, Supporting Information). Long-term survival studies further indicated that HMD(A-T) treatment produced a durable survival benefit to a majority of mice (83.3%, Figure 4k). By slice analysis of the relapsed tumors, HMD(A-T) treatment resulted in more extensive tumor cell apoptosis and microvessel destruction than all other groups (Figure S20, Supporting Information). The retrieved lungs of mice were stained, and spontaneous metastases were observed scattered in the NS, AT, and A-T groups (**Figure 5**a and b). Surprisingly, in-situ treatment of HMDs completely prevented breast cancer metastasis, ultimately improving overall survival of mice.

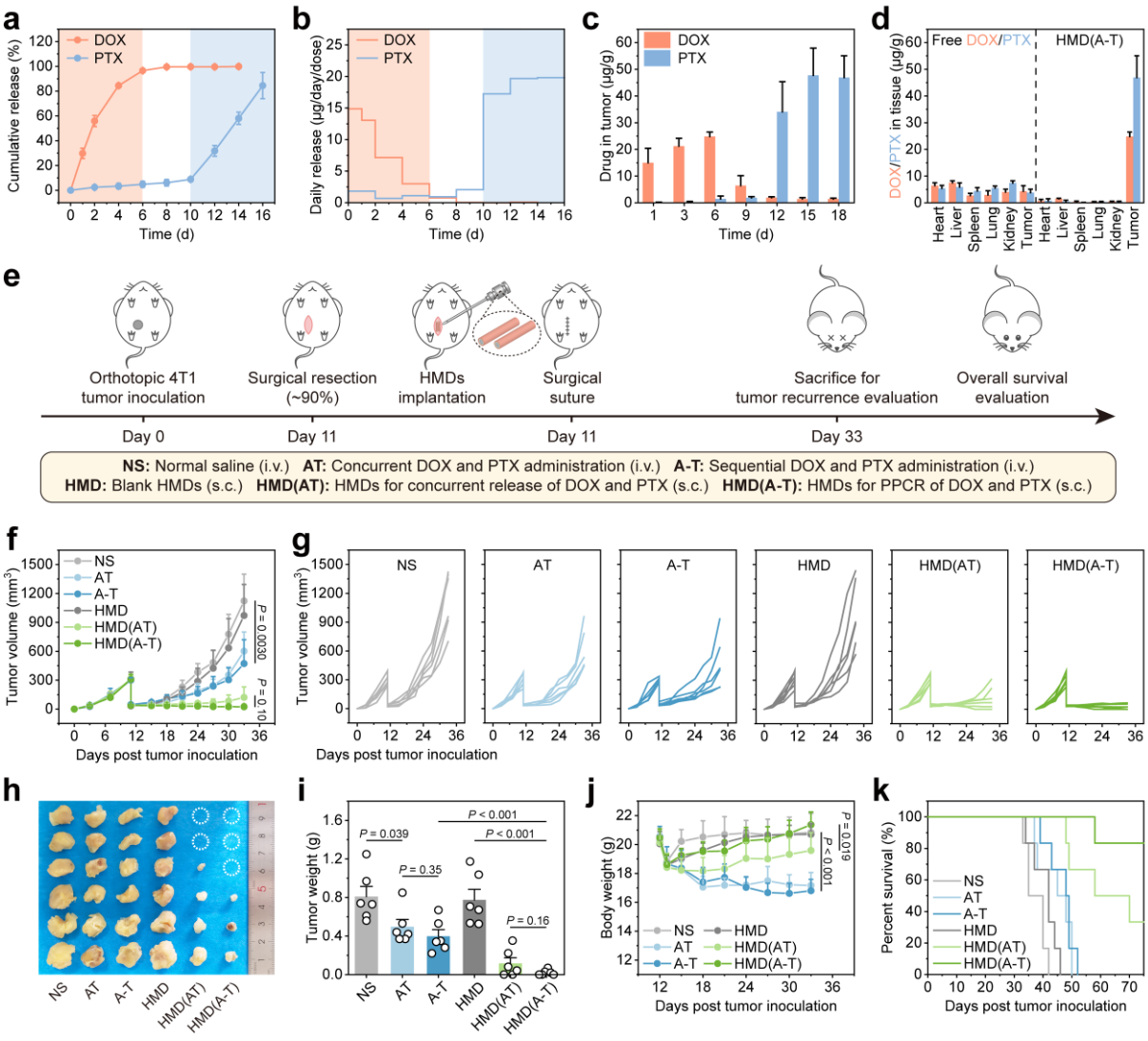

Figure 4. Engineering HMDs enabling in-situ PPCR of DOX and PTX for postsurgical breast tumor treatment. In vivo a) cumulative and b) daily drugs release profiles of HMD(A-T). c) The DOX and PTX content in tumors upon HMD(A-T) injection. d) The DOX and PTX biodistribution of i.v. free drugs administration and s.c. HMD(A-T) injection. e) Treatment scheme of surgical resection and HMD(A-T) regimen in 4T1 tumor-bearing mice. f) Average and g) individual tumor growth kinetics. h) Image and i) weight of tumors after treatment. j) Body weight changes of mice after treatment. k) Animal survival curves. For a, c, and d, data represent mean ± s.d. of n = 3 independent samples. For f and j, data represent mean ± s.d. of n = 6 independent samples. For i, data represent mean ± s.e.m. of n = 6 independent samples. Statistical significance was determined using the two-tailed unpaired *t*-test.

Orthotopic implantation of 4T1 tumors in mice boosted the count of white blood cells (WBC, Figure 5c), primarily driven by the increase of neutrophils (NEU, Figure 5d).[35] This was previously demonstrated to be associated with the metastasis of breast cancer, as NEU could drive the cell cycle progression of circulating tumor cells (CTCs) and expand their metastatic possibility.[36] Inspiringly, HMD(A-T) treatment normalized WBC and NEU levels, aligning with the tumor burden and metastasis.

Blood analysis of lactate dehydrogenase LDH-1 and creatine kinase MB activities was used to indicate any cardiac dysfunction (Figure 5e and f), and the lipid peroxide and cardiac antioxidant enzyme levels were further detected. The results confirmed that elevated myocardial oxidative damage was induced by systemic and/or concurrent administrations (Figure 5g-j), as DOX/PTX combination was suggested to aggravate the anthracycline-induced cardiotoxicity (AIC).[37] With increased local drug concentrations and reduced systemic exposure, systemic toxicity can be greatly reduced by HMD(A-T) treatment. Moreover, the local sequential release of DOX and PTX limited the overlapping toxicity by avoiding the adverse pharmacokinetic effects of their combination and reducing the myocardial metabolism of doxorubicin to the toxic doxorubicinol.[38] Therefore, compared with the AT, A-T, and HMD(AT) groups, intervention by HMD(A-T) successfully alleviated the AIC, demonstrating excellent therapeutic safety.

In addition, for many solid tumor types, a considerable number of patients are diagnosed with locally advanced disease or large tumors and may be offered preoperative administration (i.e., neoadjuvant therapy) to render surgery feasible or to make organ preservation possible.[39] Even worse, some advanced or elderly patients with unresectable tumors have to receive palliative care.[2b] Thus, an injectable device may be suitable for patients with the unresectable disease to control the localized tumor as a minimally invasive intervention.[40]

The specially fabricated mini sizes of the HMDs makes them suitable for injection into the body via needles. Therefore, to expand the application scope of the HMPI-fabricated HMDs in advanced

and unresectable cancers, HMD(A-T) was applied by s.c. injection proximal to orthotopic large-size unresectable tumors (~500 mm^3, Figure 5k).[41] The applied multi-course controlled release of DOX and PTX (DOX/PTX = 5.00/15.0 mg/kg) in situ significantly inhibited tumor growth (Figure 5l and m) without evident toxicity (Figure 5n), outperforming AT regimen and the control arms of NS and HMD. This intervention further extended the survival of mice bearing large-size tumors, half of which were still alive at day 24 after HMD(A-T) treatment (Figure 5o). Thus, the results show that the HMDs have potential implemented implications for minimally invasive treatment of unresectable tumors.

Summing up the above, the HMDs engineered by the HMPI strategy realized the sequential chemotherapy-specified controlled release of multi-drug. Borrowing a page from the clinical practice, an HMD that enables sequential release of DOX and PTX in situ showed successful preclinical applications in postsurgical and unresectable breast cancer models. Most importantly, the HMPI strategy offers an opportunity to optimize multi-drug release profiles and avoid the combined toxicity of multi-drug usage, thus representing a promising alternative for clinical combination medication.

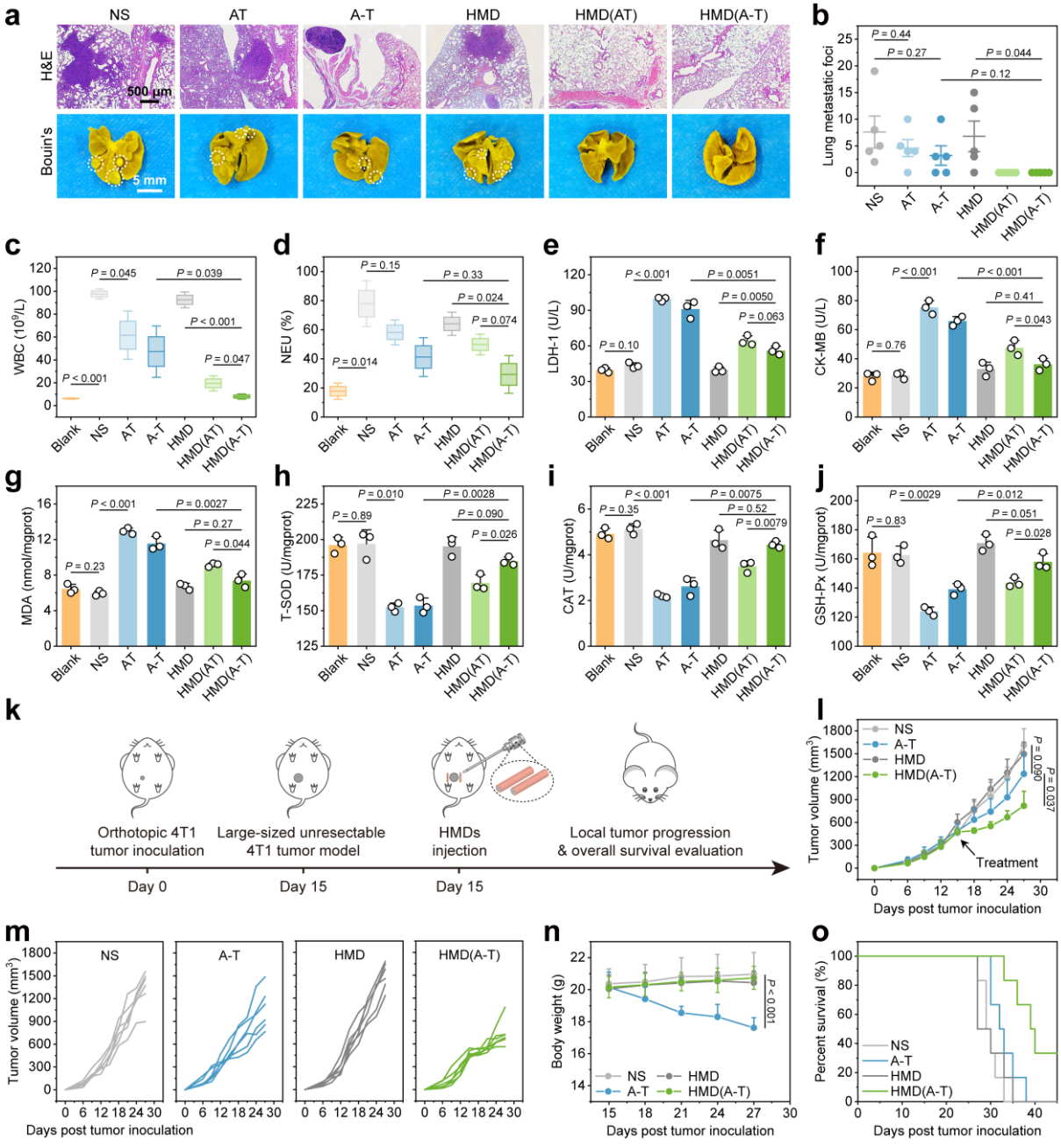

Figure 5. The evaluation of postsurgical antimetastasis and biosafety & inhibition of large-size unresectable breast tumor by HMD(A-T) treatment. a) H&E and Bouin's solution staining of representative lung tissues of mice after treatment. b) Lung metastasis foci counting. Hematological parameters of c) WBC and d) NEU of mice after treatment. Serum levels of e) LDH-1 and f) CK-MB in mice after treatment. Cardiac lipid peroxide level of g) malondialdehyde (MDA) and antioxidant

enzyme activities of h) total superoxide dismutase (T-SOD), i) catalase (CAT), and j) glutathione peroxidase (GSH-Px) in mice after treatment. k) Treatment scheme of HMD(A-T) injection in large-size unresectable 4T1 tumor-bearing mice. l) Average and m) individual tumor growth kinetics. n) Body weight changes of mice after treatment. o) Animal survival curves. For b, data represent mean ± s.e.m. of n = 5 independent samples. For c and d, data represent mean ± s.d. of n = 3 independent samples. For e-j, data represent mean ± s.e.m. of n = 3 independent samples. For l and n, data represent mean ± s.d. of n = 6 independent samples. Statistical significance was determined using the two-tailed unpaired *t*-test.

3. Conclusion

Here we have developed a microfabrication concept (HMPI) by using an optimized set of processing methods, microstructures, and biodegradable polymers. Our study provides a proof-of-concept that the drug release from the engineered HMDs by using the HMPI strategy is a function of the geometric microstructures. As a result, hierarchical microstructures can be tailored to pre-program the drug release profiles. The clinical regimens-specified PPCR of single-drug (GEM) and multi-drug (DOX/PTX) in situ for multiple courses was presented by elaborately designing the HMDs, and their efficacy and safety were demonstrated in preclinical pancreatic and breast cancer models, respectively.

The HMPI microfabrication strategy proposed in this study allows us to create high-resolution hierarchical polymer microstructures that are difficult to produce using traditional techniques. This solves the problem of precisely controlling or programming drug release using conventional drug delivery systems, which may ultimately provide highly tolerable and effective treatment options for patients who cannot bear systemic administration after surgery and those with advanced-stage tumors that cannot be resected. This versatile strategy can further be leveraged to create additional in-situ drug controlled release profiles customized by clinical medication schedules not addressed here and explore optimized monotherapies or combination therapies in many other disease types.

Supporting Information

Supporting Information is available from the Wiley Online Library or from the author.

Acknowledgements

The authors are grateful to National Key R&D Program of China (2020YFA0710800), National Natural Science Foundation of China (32271467 and 32071364), Key Project at Central Government Level: The Ability Establishment of Sustainable Use for Valuable Chinese Medicine Resources (2060302), Key R&D Plan of Jiangsu Province (BE2018010-3), and Priority Academic Program Development of Jiangsu Higher Education Institutions (PAPD).

Received: ((will be filled in by the editorial staff))
Revised: ((will be filled in by the editorial staff))
Published online: ((will be filled in by the editorial staff))

References

[1] a)M. Horowitz, E. Neeman, E. Sharon, S. Ben-Eliyahu, *Nat. Rev. Clin. Oncol.* **2015**, 12, 213; b)O. Strobel, J. Neoptolemos, D. Jäger, M. W. Büchler, *Nat. Rev. Clin. Oncol.* **2019**, 16, 11; c)J. E. Chaft, Y. Shyr, B. Sepesi, P. M. Forde, *J. Clin. Oncol.* **2022**, 40, 546.

[2] a)H. Zeng, X. Ran, L. An, R. Zheng, S. Zhang, J. S. Ji, Y. Zhang, W. Chen, W. Wei, J. He, *The Lancet Public Health* **2021**, 6, e877; b)C. Zimmermann, N. Swami, M. Krzyzanowska, B. Hannon, N. Leighl, A. Oza, M. Moore, A. Rydall, G. Rodin, I. Tannock, A. Donner, C. Lo, *The Lancet* **2014**, 383, 1721.

[3] N. F. Ponde, D. Zardavas, M. Piccart, *Nat. Rev. Clin. Oncol.* **2019**, 16, 27.

[4] S. Senapati, A. K. Mahanta, S. Kumar, P. Maiti, *Signal. Transduct. Target. Ther.* **2018**, 3, 7.

[5] E. Blanco, H. Shen, M. Ferrari, *Nat. Biotechnol.* **2015**, 33, 941.

[6] S. Wilhelm, A. J. Tavares, Q. Dai, S. Ohta, J. Audet, H. F. Dvorak, W. C. W. Chan, *Nat. Rev. Mater.* **2016**, 1, 16014.

[7] Q. Shang, Y. Dong, Y. Su, F. Leslie, M. Sun, F. Wang, *Adv. Drug Del. Rev.* **2022**, 185, 114308.

[8] a)W. Li, J. Tang, D. Lee, T. R. Tice, S. P. Schwendeman, M. R. Prausnitz, *Nat. Rev. Mater.* **2022**, 7, 406; b)H. Abdelkader, Z. Fathalla, A. Seyfoddin, M. Farahani, T. Thrimawithana, A. Allahham, A. W. G. Alani, A. A. Al-Kinani, R. G. Alany, *Adv. Drug Del. Rev.* **2021**, 177, 113957.

[9] a)N. Myung, S. Jin, H. J. Cho, H.-W. Kang, *J. Control. Release* **2022**, 352, 685; b)M. K. Gupta, F. Meng, B. N. Johnson, Y. L. Kong, L. Tian, Y.-W. Yeh, N. Masters, S. Singamaneni, M. C. McAlpine, *Nano Lett.* **2015**, 15, 5321; c)Y. Sun, S. Soh, *Adv. Mater.* **2015**, 27, 7847.

[10] a)W. Li, J. Chen, S. Zhao, T. Huang, H. Ying, C. Trujillo, G. Molinaro, Z. Zhou, T. Jiang, W. Liu, L. Li, Y. Bai, P. Quan, Y. Ding, J. Hirvonen, G. Yin, H. A. Santos, J. Fan, D. Liu, *Nat. Commun.* **2022**, 13, 1262; b)W. Xu, P. A. Ledin, Z. Iatridi, C. Tsitsilianis, V. V. Tsukruk, *Angew. Chem. Int. Ed.* **2016**, 55, 4908; c)J. Wei, X.-J. Ju, X.-Y. Zou, R. Xie, W. Wang, Y.-M. Liu, L.-Y. Chu, *Adv. Funct. Mater.* **2014**, 24, 3312.

[11] a)M. Nash Amanda, I. Jarvis Maria, S. Aghlara-Fotovat, S. Mukherjee, A. Hernandez, D. Hecht Andrew, D. Rios Peter, S. Ghani, I. Joshi, D. Isa, Y. Cui, S. Nouraein, Z. Lee Jared, C. Xu, Y. Zhang David, A. Sheth Rahul, W. Peng, J. Oberholzer, A. Igoshin Oleg, A. Jazaeri Amir, O. Veiseh, *Sci. Adv.* **2022**, 8, eabm1032; b)X. Liu, W. Zhang, Y. Wang, Y. Chen, J. Xie, J. Su, C. Huang, *J. Control. Release* **2020**, 320, 201; c)X. Li, F. Xu, Y. He, Y. Li, J. Hou, G. Yang, S. Zhou, *Adv. Funct. Mater.* **2020**, 30, 2004851.

[12] a)M. Sarmadi, C. Ta, A. M. VanLonkhuyzen, D. C. De Fiesta, M. Kanelli, I. Sadeghi, A. M. Behrens, B. Ingalls, N. Menon, J. L. Daristotle, J. Yu, R. Langer, A. Jaklenec, *Sci. Adv.* **2022**, 8, eabn5315; b)K. T. M. Tran, T. D. Gavitt, N. J. Farrell, E. J. Curry, A. B. Mara, A. Patel, L. Brown, S. Kilpatrick, R. Piotrowska, N. Mishra, S. M. Szczepanek, T. D. Nguyen, *Nat. Biomed. Eng.* **2021**, 5, 998; c)X. Lu, L. Miao, W. Gao, Z. Chen, K. J. McHugh, Y. Sun, Z. Tochka, S. Tomasic, K. Sadtler, A. Hyacinthe, Y. Huang, T. Graf, Q. Hu, M. Sarmadi, R. Langer, D. G. Anderson, A. Jaklenec, *Sci. Transl. Med.* **2020**, 12, eaaz6606; d)K. J. McHugh, T. D. Nguyen, A. R. Linehan, D. Yang, A. M. Behrens, S. Rose, Z. L.

Tochka, S. Y. Tzeng, J. J. Norman, A. C. Anselmo, X. Xu, S. Tomasic, M. A. Taylor, J. Lu, R. Guarecuco, R. Langer, A. Jaklenec, *Science* **2017**, 357, 1138.

[13] a)K. Battiston, I. Parrag, M. Statham, D. Louka, H. Fischer, G. Mackey, A. Daley, F. Gu, E. Baldwin, B. Yang, B. Muirhead, E. A. Hicks, H. Sheardown, L. Kalachev, C. Crean, J. Edelman, J. P. Santerre, W. Naimark, *Nat. Commun.* **2021**, 12, 2875; b)B. R. Freedman, A. Kuttler, N. Beckmann, S. Nam, D. Kent, M. Schuleit, F. Ramazani, N. Accart, A. Rock, J. Li, M. Kurz, A. Fisch, T. Ullrich, M. W. Hast, Y. Tinguely, E. Weber, D. J. Mooney, *Nat. Biomed. Eng.* **2022**, 6, 1167.

[14] L. Huang, Y. Zhang, Y. Li, F. Meng, H. Li, H. Zhang, J. Tu, C. Sun, L. Luo, *Nano-Micro Lett.* **2021**, 13, 141.

[15] a)Q. Chen, Z. Xiao, C. Wang, G. Chen, Y. Zhang, X. Zhang, X. Han, J. Wang, X. Ye, M. R. Prausnitz, S. Li, Z. Gu, *ACS Nano* **2022**, 16, 18223; b)X. Ji, D. Guo, J. Ma, M. Yin, Y. Yu, C. Liu, Y. Zhou, J. Sun, Q. Li, N. Chen, C. Fan, H. Song, *Adv. Mater.* **2021**, 33, 2100949; c)R. Sun, X. Song, K. Zhou, Y. Zuo, R. Wang, O. Rifaie-Graham, D. Peeler, R. Xie, Y. Leng, H. Geng, G. Brachi, Y. Ma, Y. Liu, L. Barron, M. M. Stevens, *Adv. Mater.* **2023**, 35, 2207791.

[16] S. C. Ligon, R. Liska, J. Stampfl, M. Gurr, R. Mülhaupt, *Chem. Rev.* **2017**, 117, 10212.

[17] C. Li, C. Guo, V. Fitzpatrick, A. Ibrahim, M. J. Zwierstra, P. Hanna, A. Lechtig, A. Nazarian, S. J. Lin, D. L. Kaplan, *Nat. Rev. Mater.* **2020**, 5, 61.

[18] a)X. Xie, Y. Hu, T. Ye, Y. Chen, L. Zhou, F. Li, X. Xi, S. Wang, Y. He, X. Gao, W. Wei, G. Ma, Y. Li, *Nat. Biomed. Eng.* **2020**, 5, 414; b)D. Di Mascolo, A. L. Palange, R. Primavera, F. Macchi, T. Catelani, F. Piccardi, R. Spanò, M. Ferreira, R. Marotta, A. Armirotti, A. L. Gallotti, R. Galli, C. Wilson, G. A. Grant, P. Decuzzi, *Nat. Nanotechnol.* **2021**, 16, 820.

[19] S. M. Li, H. Garreau, M. Vert, *J. Mater. Sci. Mater. Med.* **1990**, 1, 123.

[20] a)A. Kirillova, T. R. Yeazel, D. Asheghali, S. R. Petersen, S. Dort, K. Gall, M. L. Becker, *Chem. Rev.* **2021**, 121, 11238; b)Y. Xu, C.-S. Kim, D. M. Saylor, D. Koo, *J. Biomed. Mater. Res. B* **2017**, 105, 1692; c)V. B. Pokharkar, S. Sivaram, *J. Control. Release* **1996**, 41, 157; d)C. G. Pitt, A. R. Jeffcoat, R. A. Zweidinger, A. Schindler, *J. Biomed. Mater. Res.* **1979**, 13, 497.

[21] W. Yu, E. Maynard, V. Chiaradia, M. C. Arno, A. P. Dove, *Chem. Rev.* **2021**, 121, 10865.

[22] L. Wu, Y. Wang, X. Zhao, H. Mao, Z. Gu, *Biomacromolecules* **2023**, 24, 921.

[23] L. Yang, J. Li, W. Zhang, Y. Jin, J. Zhang, Y. Liu, D. Yi, M. Li, J. Guo, Z. Gu, *Polym. Degrad. Stab.* **2015**, 122, 77.

[24] N. Kamaly, B. Yameen, J. Wu, O. C. Farokhzad, *Chem. Rev.* **2016**, 116, 2602.

[25] R. Langer, *Chem. Eng. Commun.* **1980**, 6, 1.

[26] S. Borandeh, B. van Bochove, A. Teotia, J. Seppälä, *Adv. Drug Del. Rev.* **2021**, 173, 349.

[27] E. Moysan, G. Bastiat, J.-P. Benoit, *Mol. Pharm.* **2013**, 10, 430.

[28] a)J. Ciccolini, L. Dahan, N. André, A. Evrard, M. Duluc, A. Blesius, C. Yang, S. Giacometti, C. Brunet, C. Raynal, A. Ortiz, N. Frances, A. Iliadis, F. Duffaud, J.-F. Seitz, C. Mercier, *J. Clin. Oncol.* **2009**, 28, 160; b)C. Serdjebi, J.-F. Seitz, J. Ciccolini, M. Duluc, E. Norguet, F. Fina, B. Lacarelle, L. H. Ouafik, L. Dahan, *Pharmacogenomics* **2013**, 14, 1047.

[29] G. Veerman, V. W. T. R. van Haperen, J. B. Vermorken, P. Noordhuis, B. J. M. Braakhuis, H. M. Pinedo, G. J. Peters, *Cancer Chemother. Pharmacol.* **1996**, 38, 335.

[30] a)M. A. Heinrich, A. M. R. H. Mostafa, J. P. Morton, L. J. A. C. Hawinkels, J. Prakash, *Adv. Drug Del. Rev.* **2021**, 174, 265; b)T. N. D. Pham, M. A. Shields, C. Spaulding, D. R. Principe, B. Li, P. W. Underwood, J. G. Trevino, D. J. Bentrem, H. G. Munshi, *Cancers* **2021**, 13, 440.

[31] S. Loibl, P. Poortmans, M. Morrow, C. Denkert, G. Curigliano, *The Lancet* **2021**, 397, 1750.

[32] J. R. Mackey, T. Pienkowski, J. Crown, S. Sadeghi, M. Martin, A. Chan, M. Saleh, S. Sehdev, L. Provencher, V. Semiglazov, M. F. Press, G. Sauter, M. Lindsay, V. Houe, M. Buyse, P. Drevot, S. Hitier, S. Bensfia, W. Eiermann, O. Translational Res, B. Breast Canc Int Res Grp, *Ann. Oncol.* **2016**, 27, 1041.

[33] R. Gray, R. Bradley, J. Braybrooke, Z. Liu, R. Peto, L. Davies, D. Dodwell, P. McGale, H. Pan, C. Taylor, W. Barlow, J. Bliss, P. Bruzzi, D. Cameron, G. Fountzilas, S. Loibl, J. Mackey, M. Martin, L.

Del Mastro, V. Möbus, V. Nekljudova, S. De Placido, S. Swain, M. Untch, K. I. Pritchard, J. Bergh, L. Norton, C. Boddington, J. Burrett, M. Clarke, C. Davies, F. Duane, V. Evans, L. Gettins, J. Godwin, R. Hills, S. James, H. Liu, E. MacKinnon, G. Mannu, T. McHugh, P. Morris, S. Read, Y. Wang, Z. Wang, P. Fasching, N. Harbeck, P. Piedbois, M. Gnant, G. Steger, A. Di Leo, S. Dolci, P. Francis, D. Larsimont, J. M. Nogaret, C. Philippson, M. Piccart, S. Linn, P. Peer, V. Tjan-Heijnen, S. Vliek, J. Mackey, D. Slamon, J. Bartlett, V. H. Bramwell, B. Chen, S. Chia, K. Gelmon, P. Goss, M. Levine, W. Parulekar, J. Pater, E. Rakovitch, L. Shepherd, D. Tu, T. Whelan, D. Berry, G. Broadwater, C. Cirrincione, H. Muss, R. Weiss, Y. Shan, Y. F. Shao, X. Wang, B. Xu, D.-B. Zhao, H. Bartelink, N. Bijker, J. Bogaerts, F. Cardoso, T. Cufer, J.-P. Julien, P. Poortmans, E. Rutgers, C. van de Velde, E. Carrasco, M. A. Segui, J. U. Blohmer, S. Costa, B. Gerber, C. Jackisch, G. von Minckwitz, M. Giuliano, M. De Laurentiis, C. Bamia, G.-A. Koliou, D. Mavroudis, R. A'Hern, P. Ellis, L. Kilburn, J. Morden, J. Yarnold, M. Sadoon, A. H. Tulusan, S. Anderson, G. Bass, J. Costantino, J. Dignam, B. Fisher, C. Geyer, E. P. Mamounas, S. Paik, C. Redmond, D. L. Wickerham, M. Venturini, C. Bighin, S. Pastorino, P. Pronzato, M. R. Sertoli, T. Foukakis, K. Albain, R. Arriagada, E. Bergsten Nordström, F. Boccardo, E. Brain, L. Carey, A. Coates, R. Coleman, C. Correa, J. Cuzick, N. Davidson, M. Dowsett, M. Ewertz, J. Forbes, R. Gelber, A. Goldhirsch, P. Goodwin, D. Hayes, C. Hill, J. Ingle, R. Jagsi, W. Janni, H. Mukai, Y. Ohashi, L. Pierce, V. Raina, P. Ravdin, D. Rea, M. Regan, J. Robertson, J. Sparano, A. Tutt, G. Viale, N. Wilcken, N. Wolmark, W. Wood, M. Zambetti, *The Lancet* **2019**, 393, 1440.

[34] R. Simon, L. Norton, *Nat. Clin. Pract. Oncol.* **2006**, 3, 406.

[35] E. M. Mastria, L. Y. Cai, M. J. Kan, X. Li, J. L. Schaal, S. Fiering, M. D. Gunn, M. W. Dewhirst, S. K. Nair, A. Chilkoti, *J. Control. Release* **2018**, 269, 364.

[36] B. M. Szczerba, F. Castro-Giner, M. Vetter, I. Krol, S. Gkountela, J. Landin, M. C. Scheidmann, C. Donato, R. Scherrer, J. Singer, C. Beisel, C. Kurzeder, V. Heinzelmann-Schwarz, C. Rochlitz, W. P. Weber, N. Beerenwinkel, N. Aceto, *Nature* **2019**, 566, 553.

[37] D. Bovelli, G. Plataniotis, F. Roila, *Ann. Oncol.* **2010**, 21, v277.

[38] a)G. Minotti, A. Saponiero, S. Licata, P. Menna, A. M. Calafiore, G. Teodori, L. Gianni, *Clin. Cancer Res.* **2001**, 7, 1511; b)L. Gianni, L. Viganò, A. Locatelli, G. Capri, A. Giani, E. Tarenzi, G. Bonadonna, *J. Clin. Oncol.* **1997**, 15, 1906.

[39] a)W. Park, A. Chawla, E. M. O'Reilly, *JAMA* **2021**, 326, 851; b)L. Biganzoli, H. Wildiers, C. Oakman, L. Marotti, S. Loibl, I. Kunkler, M. Reed, S. Ciatto, A. C. Voogd, E. Brain, B. Cutuli, C. Terret, M. Gosney, M. Aapro, R. Audisio, *Lancet Oncol.* **2012**, 13, e148.

[40] a)S. Talebian, J. Foroughi, S. J. Wade, K. L. Vine, A. Dolatshahi-Pirouz, M. Mehrali, J. Conde, G. G. Wallace, *Adv. Mater.* **2018**, 30, 1706665; b)J. B. Wolinsky, Y. L. Colson, M. W. Grinstaff, *J. Control. Release* **2012**, 159, 14.

[41] H. Wu, D. Zhong, Z. Zhang, Y. Li, X. Zhang, Y. Li, Z. Zhang, X. Xu, J. Yang, Z. Gu, *Adv. Mater.* **2020**, 32, 1904958.

A microfabrication concept, termed Hierarchical Multiple Polymers Immobilization (HMPI), is proposed to fabricate surface-erodible hierarchical microdevices, which enable any desired controlled release profiles in situ in tumor beds according to clinical medication schedules. Specifically, hierarchical microdevices are tailed to implement multiple courses of single-drug and multi-drug controlled release and demonstrated promising alternative options for postsurgical and unresectable tumor control.

Lihuang Wu, Junhua Li, Yuqi Wang, Xinyue Zhao, Yiyan He, Hongli Mao*, Wenbo Tang, Rong Liu, Kui Luo, and Zhongwei Gu*

Engineered hierarchical microdevices enable pre-programmed controlled release for postsurgical and unresectable cancer treatment

ToC figure